Membrane domains and flagellar pocket boundaries are influenced by the cytoskeleton in African trypanosomes

Catarina Gadelha[a], Stephen Rothery[b], Mary Morphew[c], J. Richard McIntosh[c,1], Nicholas J. Severs[b], and Keith Gull[a,1]

[a]Sir William Dunn School of Pathology, University of Oxford, Oxford OX1 3RE, United Kingdom; [b]National Heart and Lung Institute, Imperial College, London SW3 6LY, United Kingdom; and [c]Boulder Laboratory for 3D Electron Microscopy of Cells, University of Colorado, Boulder, CO 80309

Contributed by J. Richard McIntosh, August 15, 2009 (sent for review July 14, 2009)

A key feature of immune evasion for African trypanosomes is the functional specialization of their surface membrane in an invagination known as the flagellar pocket (FP), the cell's sole site of endocytosis and exocytosis. The FP membrane is biochemically distinct yet continuous with those of the cell body and the flagellum. The structural features maintaining this individuality are not known, and we lack a clear understanding of how extracellular components gain access to the FP. Here, we have defined domains and boundaries on these surface membranes and identified their association with internal cytoskeletal features. The FP membrane appears largely homogeneous and uniformly involved in endocytosis. However, when endocytosis is blocked, receptor-mediated and fluid-phase endocytic markers accumulate specifically on membrane associated with four specialized microtubules in the FP region. These microtubules traverse a distinct boundary and associate with a channel that connects the FP lumen to the extracellular space, suggesting that the channel is the major transport route into the FP.

electron tomography | endocytosis | freeze fracture | *Trypanosoma brucei* | flagellum

Parasitic protozoa, like many cells, organize their surface membranes into subdomains or microenvironments that are specialized to accomplish particular recognition, secretory, and endocytic functions. The surfaces of parasitic organisms, however, have an extra level of constraint; they must perform these vital roles while the organism avoids elimination by defensive responses mounted by the host.

The compartmentalization of surface membrane is especially interesting in African trypanosomes because of their particular parasitic lifestyle. *Trypanosoma brucei* is a flagellate protozoan that lives in the blood of mammals in an exclusively extracellular form, fully exposed to the host immune system. Survival is assisted both by rapid endocytosis that clears the entire cell surface of bound antibodies within ≈7 min (1) and through the expression of a series of immunologically distinct cell surface coats. Each coat is produced from a single GPI-anchored variant surface glycoprotein (VSG; ref. 2). Periodic switching of the expressed VSG gene from a vast silent library enables the parasite to avoid clearance by the host's adaptive immune response, hence prolonging infection and increasing the chances of transmission by the bite of a tsetse fly.

African trypanosomes maintain the VSG coat free of most invariant endocytosis receptors that could otherwise elicit an immune response from which the organism could not escape. This is achieved through specialization of the plasma membrane at the base of the flagellum to create a protected invagination, the flagellar pocket (FP), in which the invariant receptors for endocytosis and innate immune evasion are concentrated (3, 4). The FP is the sole site for all endocytosis and exocytosis, and along with this critical function, it also plays important roles in protein and lipid sorting and recycling (for review, see ref. 5).

The FP membrane is continuous with the membranes of both the cell body and the flagellum, but it is functionally and biochemically distinct from each (3). Little is currently known about the factors that maintain this specialization, but it is likely that the cytoskeleton plays a defining role (6). Cytoskeletal elements that associate with the FP include a set of four specialized microtubules (4MT) that originates near the base of the flagellum (between the basal body and probasal body), runs around the FP, and inserts into a subpellicular array of microtubules at the junction between the FP and plasma membrane (6). This region is characterized by a narrowing of the FP at its apical end until it is little larger in diameter than the flagellum. Again, the cytoskeleton appears central to this: in particular, an electron-dense structure called the "collar" can be seen on the cytoplasmic side of this region, and ablation of a protein that localizes to this structure disrupts FP morphogenesis (7).

Because of its central importance to pathogenicity, the endocytic activity of *T. brucei* has long been studied by using well-defined markers for endocytosis and subcellular compartments (1, 8–19). These studies have established the speed, timing, and routes of uptake and traffic within the cell (1, 16, 18, 20), but a number of critical questions remain unanswered. First, given the constriction of the FP at its junction with the cell body membrane, how do molecules in the extracellular milieu gain access to its lumen? Second, is the FP compartmentalized into specialized subdomains to efficiently and simultaneously perform endocytosis, exocytosis, sorting, and recycling? Third, how is the FP membrane organization affected by the underlying cytoskeleton? Fourth, what and where are the boundary elements that define the edges of the continuous surface membrane regions?

In this article, we describe results from the use of fast, isothermal fixation along with electron tomography to create 3D views of unperturbed endocytosis occurring in the FP of bloodstream-form *T. brucei*. We then used freeze-fracture electron microscopy to search for functional compartmentalization of the FP into domains defined by particular configurations of intramembrane particles or boundary elements. When internalization is blocked, markers for fluid-phase and receptor-mediated endocytosis accumulate on a novel membrane domain that is closely associated with a subset of microtubules and marks a continuous channel linking the outside of the cell to the FP lumen.

Results

Multiple Markers for Endocytosis Accumulate on FP Membranes near the 4MT. To test the hypothesis of FP functional compartmentalization, we mapped the localization of endocytosis markers before their internalization. This is difficult to achieve in actively endocy-

Author contributions: C.G., N.J.S., and K.G. designed research; C.G., S.R., and M.M. performed research; J.R.M. contributed new reagents/analytic tools; C.G., J.R.M., and K.G. analyzed data; and C.G., J.R.M., and K.G. wrote the paper.

The authors declare no conflict of interest.

Freely available online through the PNAS open access option.

[1]To whom correspondence may be addressed. E-mail: richard.mcintosh@colorado.edu or keith.gull@path.ox.ac.uk.

This article contains supporting information online at www.pnas.org/cgi/content/full/0909289106/DCSupplemental.

CELL BIOLOGY

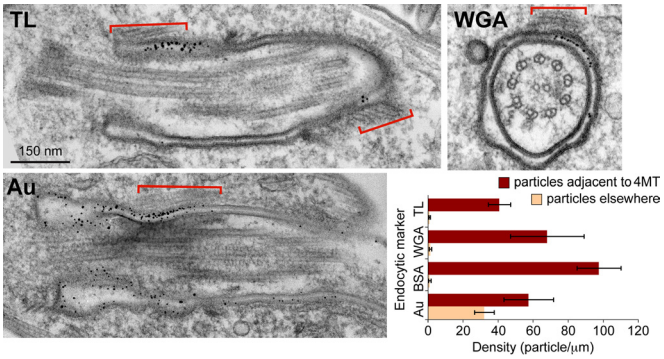

Fig. 1. When endocytosis is blocked by cold treatment of bloodstream-form trypanosomes, markers for endocytosis accumulate specifically at the membrane abutting the 4MT. Representative thin sections of the FP of cells incubated for 15 min on ice with 5-nm gold conjugated to TL or WGA, or unconjugated 5-nm gold (Au). Red bars indicate the positions at which the 4MT pass through the section. Graph shows densities of gold particles on the membrane adjacent to the 4MT or elsewhere (expressed as particles per micrometer of membrane observable in thin section). Bars represent standard errors of the mean.

tosing cells, given the extremely high rates of endocytosis. However, at <4 °C, markers for endocytosis will enter the FP from the surrounding medium, but endocytosis is blocked (11). This allows loading of the FP with the concentrations of markers necessary for ultrastructural studies.

We examined the localization of tomato lectin (TL)-binding sites in the FP of cells held at 0 °C and then rapidly fixed. TL binds tri-*N*-acetylglucosamine and specifically labels glycoproteins enriched in both the FP and endosomes of trypanosomes (21, 22). This labeling revealed a clear bias in the localization toward particular sites (Fig. 1). Gold particles preferentially accumulated on the membrane directly abutting the set of 4MT that are nucleated at the basal body and run alongside the FP. Analysis of multiple thin sections through many FPs ($n > 110$), either deep within the organelle or more distally, consistently demonstrated this to be the case. A similar accumulation was observed for gold-conjugated wheat-germ agglutinin (WGA; a lectin with a sugar specificity similar to that of TL; Fig. 1). The same localization was also found for BSA (Fig. S1), which is often used as a marker of fluid-phase endocytosis in trypanosomes (12). Under these conditions, however, BSA also appears to bind preferentially to FP membrane where it associates with the 4MT.

We assessed the preference of gold conjugates for this region by quantifying the frequency with which gold particles are associated with different parts of the FP membrane. The segment of membrane that apposes the 4MT is ≈11% of the FP perimeter, as seen in thin-section electron micrographs. If binding were stochastic, only ≈1/10 of all bound gold conjugates should be associated with membrane overlying the 4MT. The distribution in a set of representative micrographs revealed that the observed ratio is ≈3:1 in favor of 4MT association (n = 52:7, 32:12, and 38:16 for TL, WGA, and BSA, respectively). This bias is extremely unlikely to be caused by chance ($P < 10^{-10}$ for all conjugates; χ^2 test). When all of the lengths of membrane associated with the 4MT and the remainder of the FP are considered, there is a ≈60-fold higher density of gold conjugates associated with membrane abutting the 4MT than elsewhere in the FP (P = 0.0002, 0.02, and 0.001 for TL, WGA and BSA, respectively; t test; Fig. 1).

The accumulation of gold conjugates on membrane that abuts the 4MT was not caused by the gold particles themselves, because 5-nm colloidal gold alone was more homogeneously distributed (Fig. 1). We observed no significant difference in the density of particles above the 4MT compared with that elsewhere (P = 0.12; t test; Fig. 1). This difference between conjugated and unconjugated was not a consequence of the relatively larger size of the former (the estimated diameter of 5-nm gold particle conjugated to two to three molecules of BSA is ≈9 nm, whereas to TL or WGA it is ≈10 nm), because identical experiments conducted with 10-, 15-, or 20-nm gold colloids showed the same distribution as did 5 nm alone.

Clathrin-Mediated Endocytosis Is Not Regionalized in the FP. The data above show that when endocytosis is blocked a clear microdomain of the FP membrane is revealed, with endocytic markers accumulating specifically on the membrane overlying the 4MT. The presence of the microtubules might be predicted to prevent vesicle budding/docking in this region of membrane at physiological temperatures. We therefore investigated the sites of endocytosis on the FP by looking for the formation of clathrin-coated pits because clathrin-mediated endocytosis appears to be the only mode of internalization in these parasites (1, 23).

To analyze cells in which endocytosis was fully active, we rapidly fixed cells at 37 °C while they were still in their culture flasks, then subjected them to serial-section, dual-axis electron tomography. We produced 3D reconstructions of a large proportion of the posterior end of bloodstream-form trypanosomes at a resolution of ≈5 nm. This volume encompasses the full FP, its associated cytoskeleton, and the surrounding membranous organelles. The quality of the structural preservation, and the resolution of the tomographic slices used in this study, are demonstrated in Fig. 2*A*. The corresponding 3D reconstruction is shown in Movie S1; segmented models of the FP and its surrounding organelles are shown in Fig. 2*B*, Movie S2, and Movie S3. The resolution of our tomographic reconstructions is such that the clathrin polygons indicative of endocytosis are readily identifiable (Fig. 3), and

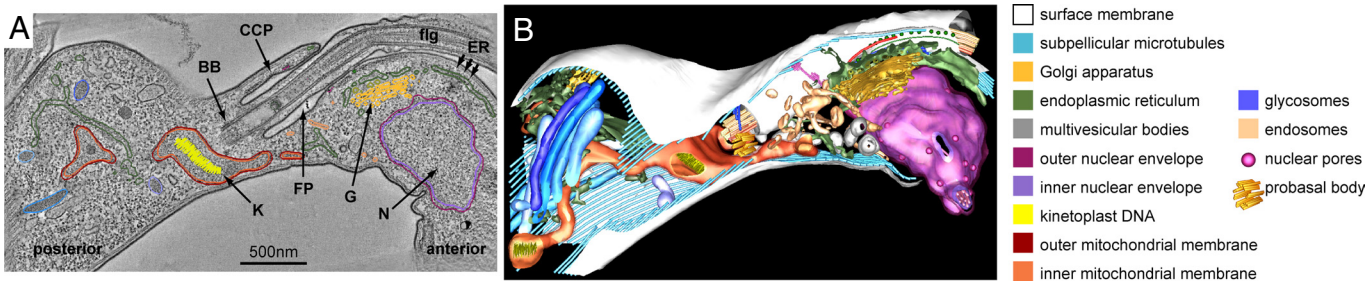

Fig. 2. Electron tomographic reconstruction used to model an entire FP, surrounding organelles, and cytoskeleton. (*A*) A single ≈2-nm slice from a 250-nm-thick serial-section 3D reconstruction of the anterior FP region from a late M-phase bloodstream-form trypanosome with some of the structures modeled by segmentation along organelle contours. The FP can be seen clearly near the center of the slice, as can the anterior kinetoplast (K), Golgi (G), and the dividing nucleus (N). The anterior–posterior polarity of the trypanosome cell (defined by its swimming direction) is also indicated. The full reconstruction can be seen in Movie S1. (*B*) A full 3D segmentation model formed from the serial-section reconstruction by the process shown in *A*. The relationships between individual structures can now be seen clearly. This segmentation model can also be seen in Movie S2 and Movie S3.

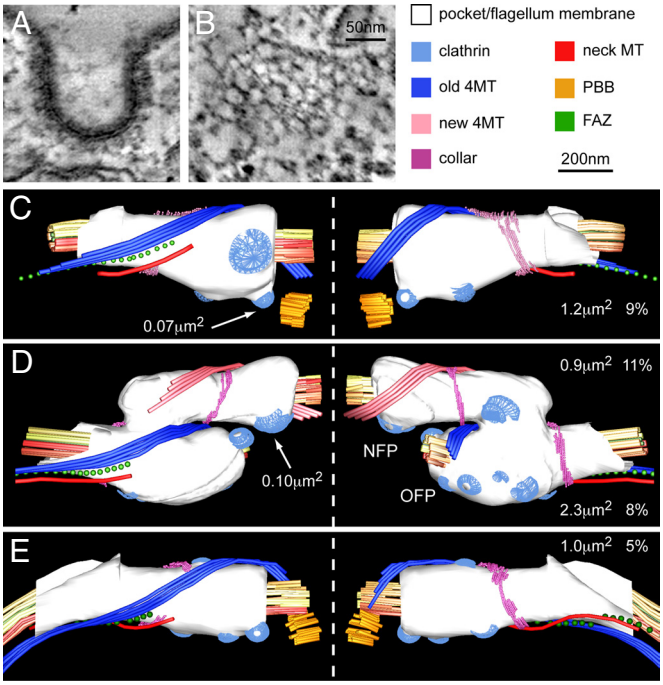

Fig. 3. Clathrin structures seen in tomographic reconstructions of the trypanosome FP. (*A* and *B*) Both highly curved pits (*A*) and also flatter areas (*B*) can be seen (images are 5-nm tomographic slices from tomograms). Clathrin triskelion assembly is not seen near the 4MT or at the collar. No gross segregation to particular subdomains is observed. (*C–E*) FP topography from segmentation models of electron tomographic reconstructions of whole FP in cells in G_1 (*C*), nuclear S phase (*D*), or late mitosis (*E*). Patches of clathrin assembly are shown in light blue, along with the 4MT (dark blue), the collar (pink), and FAZ maculae (green). The newly identified microtubule associated with the neck region is also shown (red). The total surface area of the FP and the percentage that is coated by clathrin are indicated on the right of each panel. The surface area of some individual clathrin-coated pits are also indicated by white arrows. In *D*, NFP and OFP indicate new and old FPs, respectively.

clathrin structures are seen associated with deeply curved pits (Fig. 3*A*) and as flatter lattices (Fig. 3*B*).

We extended our electron tomographic analysis by reconstructing posterior ends from 15 trypanosomes at different stages of the cell cycle, which allowed us to examine endocytosis during the time when the FP duplicates. Temporal classification of individual cells to particular points in the cell cycle is relatively easy in trypanosomes because of the consistent appearance of identifiable morphological changes at specific times (24). Clathrin structures could be seen throughout the cell cycle; they were equally prominent on FPs of trypanosomes in G_1 (Fig. 3*C*), nuclear S phase (Fig. 3*D*), and late mitosis (Fig. 3*E*), suggesting that endocytosis continues throughout the cell cycle. Moreover, clathrin assemblies were seen on newly formed FPs very soon after their separation from the preexisting FP (Fig. 3*D*), indicating that endocytosis initiates swiftly on the nascent FP.

To analyze the distribution of clathrin assemblies around the FP, we used external structures to create a frame of reference. The anterior side of the FP is defined as facing the anterior end of the cell (Fig. 2*A*). The area near the junction between the FP and flagellar membrane will be called the base, whereas the collar marks the uppermost border of the FP. We found no bias in the location of clathrin to specific areas of the FP in our 15 3D reconstructions. Clathrin-coated pits and sheets were observed from the base of the FP up to the collar. Clathrin assembly was also seen on both anterior and posterior sides of the FP, in contrast to the proposition that only the anterior face might be competent for endocytosis (25). Our observation was confirmed by thin-section micrographs of many

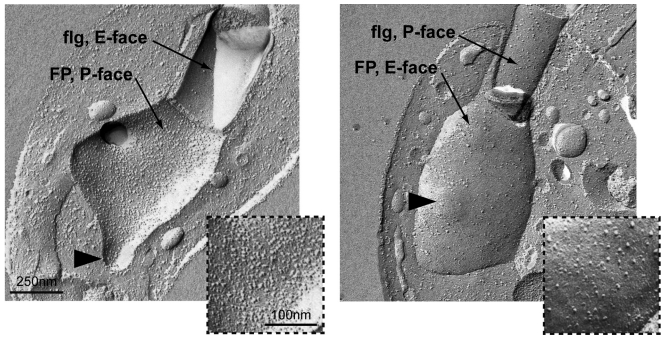

Fig. 4. Freeze fracture of the FP membrane. Note that IMPs are homogeneously distributed, with a higher numerical density on the P face than the E face. Invaginated membrane domains, representing sites of endocytosis or exocytosis, are indicated by arrowheads. Platinum/carbon shadow direction is from bottom to top. Insets show FP membrane faces at higher magnification.

FPs in which clathrin assemblies could be seen ($n = 102$). In these, the distributions of clathrin across the posterior and anterior faces of the FP were about equal (43 thin sections with clathrin on the posterior side, 49 on the anterior side, and 10 thin sections with clathrin on both sides). Support for posterior face uptake can also be found in the literature (for an example, see figure 1*a* in ref. 12).

Significantly, no clathrin was seen on the membrane directly overlying the 4MT, nor was it seen on the neck membrane (see below) or any part of the flagellar membrane. These data suggest that bloodstream-form trypanosomes have the capacity for endocytosis throughout the FP except for the portion directly associated with the 4MT and the boundary between the basal body and the axoneme. In agreement with the suggestion that all endocytosis in trypanosomes is clathrin-mediated (23), no uncoated pits or non-clathrin-coated invaginations were observed in either tomographic slices or thin-section micrographs.

A specific "neck region" of plasma membrane surrounds the flagellum at the postcollar exit point of the FP (6, 26). The 4MT rootlet remains attached to the neck region membrane but is joined there by a short microtubule and the flagellum attachment zone (FAZ) macula adherens and filament (Fig. 3 *C–E* and Movie S3).

The Distribution of Intramembrane Particles (IMPs) Within the FP Is Homogeneous. To ask whether endocytosis or other FP functions were accompanied by membrane differentiation, we analyzed freeze-fracture replicas of cells prepared after rapid isothermal fixation as above. Freeze-fracture techniques cleave cellular membranes through the central hydrophobic plane of the lipid bilayer, revealing two internal fracture faces referred to as the protoplasmic (P) face (the hydrophobic aspect of the half-membrane leaflet attached to the cytoplasm) and the extracellular (E) face (the hydrophobic aspect of the half-membrane leaflet attached to the exterior or organelle lumen). A replica of these faces exposes integral membrane proteins as IMPs (see Fig. S2*A*), allowing any membrane differentiation to be visualized (note that proteins such as VSG, which are tethered to the membrane by a GPI anchor, will not produce IMPs).

Consistent with our observation that the entire FP is endocytosis-competent, both the P face and the E faces of the FP membrane showed an essentially even distribution of IMPs (Fig. 4). As in most membranes, the P face of the FP membrane has a markedly higher density of IMPs than does the E face. These observations were consistent from cell to cell, as seen in freeze-fracture views of 80 FPs (42 P faces and 38 E faces), representing $\approx 25\ \mu m^2$ of FP membrane area. Distinct deformations of the FP, which mark sites of endocytosis/exocytosis, were present on 38 of 80 views of FPs (Fig. 4, arrowheads), and no difference in IMP distribution or density was associated with the membrane in these regions (Fig. 4). Combined

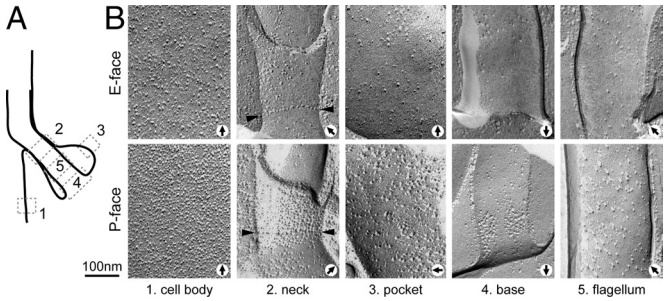

Fig. 5. The cell surface, FP, and flagellar membranes have different densities of IMPs and are separated by boundary elements with distinctive patterns of particles. Representative images of IMP density and distribution in the membrane regions illustrated by the diagram in *A* are shown in *B*. P faces and E faces of each membrane region are shown, together with views of the neck (boundary between the surface and FP membranes) and the flagellum base (boundary between the FP and flagellum membranes). Arrowheads indicate rows of IMPs at the base of the neck. Black arrows indicate direction of platinum/carbon evaporation. Note that panels are presented to match the orientation of the diagram in *A*. Magnification bar applies to all frames.

with the findings above, these data indicate that there are no identifiable subdomains within the FP on the basis of either clathrin recruitment or IMP distribution, suggesting that all parts of the organelle have an equal capacity to be involved in membrane trafficking.

The accumulation of markers for endocytosis on the membrane directly abutting the 4MT under cold conditions suggests that this specific area constitutes a differentiated domain. Indeed, a band of four helical rows of IMPs was occasionally seen on P-face views of the FP ($n = 4$; Fig. S2*B*). Although their number, helicity, angle, and interspacing suggest a relationship to the 4MT, the rarity of these fractures indicates that such a relationship is restricted to a limited distance, is transient, or that there is systematic bias against fractures through this area.

Clustered IMPs Demarcate Membrane Boundaries. The plasma, FP, and the flagellar membranes are continuous, yet their functions and biochemical composition are distinct (3). How are these distinct domains maintained on different regions of continuous membrane? We used freeze-fracture techniques to look for differential IMP distributions between the surface, FP, and flagellar membranes, paying particular attention to boundaries. The three membranes showed different IMP densities (Fig. 5), presumably reflecting their distinct composition. When analyzing the boundaries between these membranes, we found distinctive arrangements of IMPs. The junction of the surface membrane and FP (the neck region) was characterized by a distribution of IMPs on both the E and P faces that was similar to that of the cell surface but clearly denser than that found in the FP (Fig. 5*B*). In addition, at the most basal edge of the neck (the point of junction with the FP), near where the collar is found in 3D reconstructions, we observed distinct rows of IMPs on both faces (13 of 13 freeze-fracture views of this zone; Fig. 5*B*). No obvious IMP organization was seen in fractures across the flagellum exit site ($n = 41$), suggesting the absence of a membrane boundary between the distal edge of the neck region and the parasite surface.

At the base of the flagellum, P-face views revealed plaques of densely packed IMPs (≈75 nm wide, ≈180 nm long, and spaced by ≈40 nm; Fig. 5*B*); these we interpret as the flagellar plaques (27). The corresponding E-face views were devoid of detectable IMP organization. This observation was consistent through fractures across the base of 51 flagella (21 P faces and 30 E faces).

A Channel Connects the FP Lumen and the Extracellular Space. For macromolecules to be taken up by the trypanosome, they must first enter the FP across the barrier imposed by the tight apposition of the neck and flagellar membranes. How this is achieved has not been determined. Here, we have found that markers for endocytosis accumulate on the membrane abutting the 4MT when endocytosis is blocked by cold temperatures. This has led us to hypothesize that the 4MT, which traverse the neck, are involved in uptake into the FP. To test this hypothesis, we reexamined thin sections of cells that had been incubated with BSA, WGA, and TL 5-nm gold conjugates at 0 °C (Fig. 1), analyzing both cytoskeletal structure and marker binding in this neck region. The occurrence of gold particles on the membrane directly abutting the 4MT was seen in multiple thin sections along the length of the neck, and in sections through the site of flagellum exit from the cell (Fig. 6). In the neck, the gold particles occurred in a luminal space found between the otherwise tightly apposed neck and flagellar membranes at the point defined by the 4MT.

This luminal space, which we call the "neck channel," was not caused by either the presence of gold particles or incubation of cells in cold conditions, because it was also seen in thin sections of cells fixed in the absence of gold and at physiological temperatures (Fig. S3*A*). Nor was it caused by aldehyde fixation, because it could be seen in cells cryoimmobilized by high-pressure freezing followed by freeze substitution (Fig. S3*B*).

The neck channel was observed in multiple thin sections ($n = 67$) derived from different sample preparations ($n > 10$), all of which suggested that this feature forms a continuous channel linking the FP lumen and the extracellular environment. Also, it was possible to see the continuity of the channel through the neck region in at least some of our 3D tomographic reconstructions of the FP region (Fig. S4).

Discussion

Surface Membrane Domains. The *T. brucei* surface membrane is organized into four domains: those surrounding the cell body, the neck, the FP, and the flagellum. Despite being continuous, each of these domains shows a distinct IMP density (surface ≈ neck > FP >

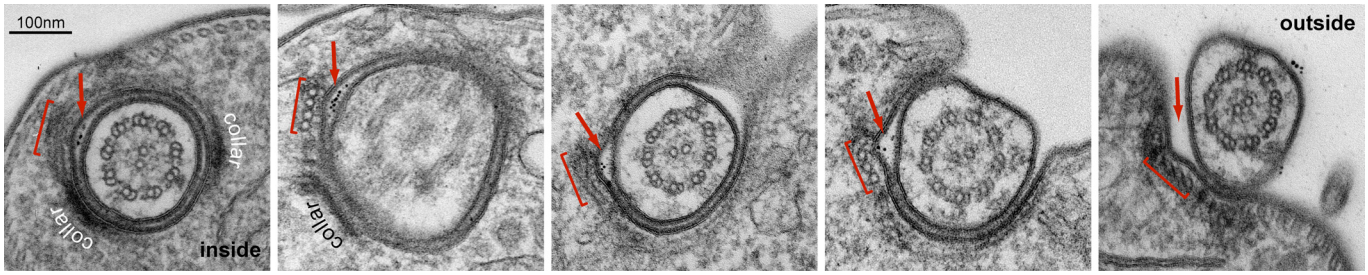

Fig. 6. The 4MT in the neck region are associated with a channel that connects the FP to the extracellular space. Transverse thin-section electron micrographs of the neck and flagellum exit site in cells incubated for 15 min on ice with TL conjugated to 5-nm gold. There is a clear accumulation of gold particles in a gap between the flagellum membrane and the neck membrane directly abutting the 4MT (red arrows). Red bars indicate the positions at which the 4MT pass through the section.

flagellum). Our observations extend previous freeze-fracture studies (28–30), emphasizing the neck membrane as a distinct cellular environment. This region is devoid of subpellicular microtubules, which could theoretically allow vesicle budding/docking, yet our data suggest that it does not perform endocytosis. We identified two structures that were unique to this surface domain: one short microtubule that appears distinct from the subpellicular array and a channel that connects the cell exterior to the interior of the FP.

Many receptors (e.g., those for transferrin and haptoglobin-hemoglobin) in trypanosomes are GPI-anchored, as is the major surface protein (VSG). This is the likely explanation for the lower density of IMPs on the FP membrane compared with either the cell body or the neck membranes. It is possible that many IMPs represent members of the invariant surface glycoprotein family that possess a single transmembrane domain and are present in high copy number (3). We did not see any differentiation of the FP membrane into subdomains on the basis of IMP distribution.

Boundaries Between Continuous Surface Domains. Our analysis shows that there are distinct structures at two of the boundaries that divide the surface membrane domains: (*i*) the flagellar plaques at the junction of the flagellum and FP membranes, and (*ii*) IMP arrays at the junction of the FP and neck membranes, presumably corresponding to the collar region. Our results extend earlier freeze-fracture studies that also recognized the likely importance of these structures in restricting membrane protein movement (26, 28, 30–32).

The amorphous, electron-dense collar is seen in thin-section micrographs in the cytoplasm at the most superficial edge of the FP. Our electron tomographic analysis revealed that the collar appears thinner or entirely absent at the point of passage of the 4MT, so it is horseshoe-shaped (7). Interpretation and modeling of the electron-dense amorphous material are difficult. However, the rows of IMPs on the neck membrane at the same position as the collar were uninterrupted on both P and E faces in our freeze-fracture analysis. These data suggest that the membrane boundary seen by freeze fracture may be coincident with, but separate from, the cytoskeletal structure of the collar.

The flagellar plaques and the collar separate the FP membrane from the continuous membranes of the cell body and flagellum, and specific surface proteins (such as receptors) are enriched on the FP membrane. FP proteins, such as the transferrin receptor (TfR), however, are similar to the VSG molecules in both tertiary structure and membrane anchorage, although their GPI valencies differ (2). Despite this, the FP boundaries appear able to discriminate between TfR and VSG, because newly synthesized/recycled VSG delivered to the FP moves out to the cell surface, whereas TfR is retained.

No Endocytosis Regionalization in the FP. The whole FP, except the membrane directly abutting the 4MT, appears able to recruit clathrin (and is thus equipped to perform endocytosis), with no evidence for FP subdomains on the basis of IMP distribution. Our electron microscopy procedures used a rapid isothermal fixation with minimal prior manipulation to try to obtain structures that would closely reflect unperturbed endocytosis. Our data argue against the proposal that endocytosis in trypanosomes is spatially limited within the FP (33). Our electron tomography brings an increased resolution in 3D to the analysis, but we cannot exclude the alternative possibilities: (*i*) endocytosis on the anterior and posterior sides of the FP differs in molecular character; (*ii*) although both anterior and posterior sides of the FP recruit clathrin and form coated pits, only the anterior side goes on to bud productive vesicles; and (*iii*) our rapid chemical fixation does not immobilize lipids, so membrane proteins randomize their positions after other cellular events have ceased, presenting us with an erroneous view of FP structure.

One of the interesting observations from our analysis of clathrin distribution on the FP is the occurrence of both curved and flat assemblies of clathrin triskelions. It has been proposed that the planar arrays are reservoirs of clathrin available for rapid recruitment into a pit (34). The extremely fast endocytic rate of the *T. brucei* FP, and its high dependency on clathrin-mediated internalization, may favor a mechanism in which the cell constantly preassembles flat lattices as clathrin reservoirs to sustain the formation of a large number of coated pits and vesicles.

Transport into the FP. The concentration of all endocytosis into the FP (35) allows the invariant receptor proteins to be sequestered in an environment that is protected from the attentions of host defenses. However, any macromolecules or complexes that are to bind FP receptors must first traverse the region in which the flagellum and neck membranes are tightly apposed. Our work has revealed a channel that runs the length of the neck and is closely associated with the 4MT. The channel represents a means by which extracellular components can gain access to the FP lumen. When cells were incubated at 0 °C with colloidal gold, conjugated to markers for either receptor-mediated or fluid-phase endocytosis, particles accumulated at high density in the channel. The 4MT appear able to provide local dislocation to membranes; a deep, longitudinal fold was also seen in the FP membrane adjacent to a group of rootlet microtubules of a related trypanosomatid, *Leishmania collosoma* (31).

The *T. brucei* neck channel is not an artifact of gold particle interaction with the cell, cold temperatures, or chemical fixation, but is consistently found in cells from a range of treatments and fixations. The finding of gold particles at high density in the neck channel but very rarely elsewhere in the neck region suggests that the channel is the major means of access to the FP lumen for extracellular components. Given the general capacity of the FP membrane to recruit clathrin, it is expected that markers for endocytosis accessing the FP through the channel would then redistribute across the FP membrane. However, when endocytosis is blocked, markers conjugated to gold remain at the membrane overlying the 4MT. This clustering is especially striking, given that this membrane is the only region of the FP that seems likely to be incompetent for endocytosis.

A previous study (10) of ricin-binding glycoproteins also showed accumulation of gold marker on the FP membrane overlying the 4MT, and the authors proposed the presence of a discrete surface domain within the organelle. Our quantitative electron microscopy extends this observation to a range of markers and emphasizes localization in the neck channel. However, it is important to consider the interpretation of this highly localized distribution and its relevance to physiological endocytosis. At 37 °C, the markers used in our studies are internalized by the trypanosome. Key questions include why these markers are clustered selectively onto the area of the 4MT domain and how they migrate from this zone so they can be internalized from other areas of the FP membrane. There are two contexts to the discussion: is the neck channel an active escalator for bound marker internalization to the FP, is it a passive free-flow conduit, or is it both? If an escalator, then one might presume that this active movement is unlikely to operate at 0 °C, but if it does then the markers must be incapable of escaping the escalator to the main membrane of the FP. If not, and entry to the FP lumen is via a passive fluid entry through the neck channel, then this would suggest either (*i*) that the receptors are congregated or more concentrated (before ligand entry or as a result of ligand binding) to only the 4MT area, or (*ii*) that any receptors located elsewhere on the FP membrane are masked at this temperature. Finally, it may be that the 4MT band acts as a cytoskeletal barrier to lateral movement of receptors. Thus, cross-linking by multivalent gold-bound markers could produce aggregates of GPI-anchored proteins and transmembrane partners that then become bound to the underlying cytoskeletal framework, as has been demonstrated in animal cells (36).

The proposed involvement of the channel and 4MT in trafficking into the FP suggests the participation of molecular motors in the movement of membrane-associated material. There are many uncharacterized motors encoded in the trypanosome genome that could be invoked (37). What, if any, selection is performed by the channel and neck region? The fact that trypanosomes take unconjugated gold into the FP lumen would suggest that there is no strong selection on the basis of molecular recognition. However, it is easy to see that a selection on the basis of size could operate at the channel. Interestingly, we have observed that 20-nm particles enter the FP, but 40-nm gold does not. A quantitative analysis of multiple thin sections showed that the smallest dimension of the channel varied from 25 to 150 nm. Such dimensions would be sufficient to allow the passage of both high- and low-density lipoprotein complexes (≈8 and 22 nm in diameter, respectively), which are scavenged by receptors in the FP. A final and critical question is how the neck and channel are involved in transport of material out of the FP. In this work, we have concentrated on movement of material into the FP, largely because the lack of a traceable marker makes it very difficult to follow secretion in the parasite. However, the fast rates of endocytosis measured for *T. brucei* imply not only a rapid flux of membrane into the FP, but a comparable flux of VSG-coated membrane out of the FP (disregarding losses from shedding of cell surface and cell growth). How these two opposing flows are organized is currently unknown. Finally, because African trypanosomes possess a flagellum at all times, what effect, if any, might the beating of the flagellum have on the closely associated channel?

Methods

Cold Uptake. Cells were harvested at 4 °C, resuspended in chilled PBS plus 20 mM glucose, and held on ice for 10 min before being pulsed for 15 min with 5-nm colloidal gold conjugated to either BSA, WGA, or TL, or with unconjugated colloidal gold. Pulse was stopped by the addition of isothermal glutaraldehyde. Please see *SI Methods* for full description.

Fast, Isothermal Fixation. Cells were fixed in culture by the addition of isothermal glutaraldehyde to the culture flask while the latter was still in the 37 °C incubator, as detailed in *SI Methods*.

High-Pressure Freezing. Cells grown in culture medium supplemented with gum arabic were high-pressure-frozen in ≈10 ms and freeze-substituted in uranyl acetate and glutaraldehyde or osmium tetroxide, as described in *SI Methods*.

Electron Tomography. Dual-axis 3D reconstructions were acquired essentially as described (6) and as detailed in *SI Methods*.

Freeze Fracture. Freeze fracture was performed by using standard techniques, as detailed in *SI Methods*.

ACKNOWLEDGMENTS. We thank Bill Wickstead for valuable discussion and Michael Shaw (University of Oxford) for electron microscopy assistance. This work was supported by the Human Frontier Science Program, Wellcome Trust, the EP Abraham Trust, and National Institutes of Health Grant RR000592 (to J.R.M.). K.G. is a Wellcome Trust Principal Research Fellow.

1. Grunfelder CG, et al. (2003) Endocytosis of a glycosylphosphatidylinositol-anchored protein via clathrin-coated vesicles, sorting by default in endosomes, and exocytosis via RAB11-positive carriers. *Mol Biol Cell* 14:2029–2040.
2. Ferguson MAJ (1999) The structure, biosynthesis, and functions of glycosylphosphatidylinositol anchors and the contributions of trypanosome research. *J Cell Sci* 112:2799–2809.
3. Borst P, Fairlamb AH (1998) Surface receptors and transporters of *Trypanosoma brucei*. *Annu Rev Microbiol* 52:745–778.
4. Vanhollebeke B, et al. (2008) A haptoglobin-hemoglobin receptor conveys innate immunity to *Trypanosoma brucei* in humans. *Science* 320:677–681.
5. Overath P, Engstler M (2004) Endocytosis, membrane recycling, and sorting of GPI-anchored proteins: *Trypanosoma brucei* as a model system. *Mol Microbiol* 53:735–744.
6. Lacomble S, et al. (2009) 3D cellular architecture of the flagellar pocket and associated cytoskeleton in trypanosomes revealed by electron microscope tomography. *J Cell Sci* 122:1081–1090.
7. Bonhivers M, Nowacki S, Landrein N, Robinson D (2008) Biogenesis of the trypanosome endo-exocytic organelle is cytoskeleton mediated. *PLoS Biol* 6:e105.
8. Balber AE (1990) The pellicle and the membrane of the flagellum, flagellar adhesion zone, and flagellar pocket: Functionally discrete surface domains of the bloodstream form of African trypanosomes. *Crit Rev Immunol* 10:177–201.
9. Balber AE, Frommel TO (1988) *Trypanosoma brucei gambiense* and *T. b. rhodesiense*: Concanavalin A binding to the membrane and flagellar pocket of bloodstream and procyclic forms. *J Protozool* 35:214–219.
10. Brickman MJ, Balber AE (1990) *Trypanosoma brucei rhodesiense* bloodstream forms: Surface ricin-binding glycoprotein are localized exclusively in the flagellar pocket and the flagellar adhesion zone. *J Protozool* 37:219–224.
11. Brickman MJ, Cook JM, Balber AE (1995) Low temperature reversibly inhibits transport from tubular endosomes to a perinuclear, acidic compartment in African trypanosomes. *J Cell Sci* 108:3611–3621.
12. Coppens I, Opperdoes F, Courtoy PJ, Baudhuin P (1987) Receptor-mediated endocytosis in the bloodstream form of *Trypanosoma brucei*. *J Protozool* 34:465–473.
13. Engstler M, et al. (2007) Hydrodynamic flow-mediated protein sorting on the cell surface of trypanosomes. *Cell* 131:505–515.
14. Grab DJ, et al. (1992) Endocytosed transferrin in African trypanosomes is delivered to lysosomes and may not be recycled. *Eur J Cell Biol* 59:398–404.
15. Hager KM, et al. (1994) Endocytosis of a cytotoxic human high-density lipoprotein results in disruption of acidic intracellular vesicles and subsequent killing of African trypanosomes. *J Cell Biol* 126:155–167.
16. Langreth SG, Balber AE (1975) Protein uptake and digestion in bloodstream and culture forms of *Trypanosoma brucei*. *J Protozool* 22:40–53.
17. Magez S, et al. (2001) A conserved flagellar pocket exposed high mannose moiety is used by African trypanosomes as a host cytokine binding molecule. *J Biol Chem* 276:33458–33464.
18. Webster P (1989) Endocytosis by African trypanosomes. 1. Three-dimensional structure of the endocytic organelles in *Trypanosoma brucei* and. *T congolense*. *Eur J Cell Biol* 49:295–302.
19. Webster P, Grab DJ (1988) Intracellular colocalization of variant surface glycoprotein and transferrin gold in *Trypanosoma brucei*. *J Cell Biol* 106:279–288.
20. Engstler M, et al. (2004) Kinetics of endocytosis and recycling of the GPI-anchored variant surface glycoprotein in *Trypanosoma brucei*. *J Cell Sci* 117:1105–1115.
21. Atrih A, Richardson JM, Prescott AR, Ferguson MAJ (2005) *Trypanosoma brucei* glycoproteins contain novel giant poly-*N*-acetyllactosamine carbohydrate chains. *J Biol Chem* 280:865–871.
22. Nolan DP, Geuskens M, Pays E (1999) N-linked glycans containing linear poly-*N*-acetyllactosamine as sorting signals in endocytosis in *Trypanosoma brucei*. *Curr Biol* 9:1169–1172.
23. Allen CL, Goulding D, Field MC (2003) Clathrin-mediated endocytosis is essential in *Trypanosoma brucei*. *EMBO J* 22:4991–5002.
24. Woodward R, Gull K (1990) Timing of nuclear and kinetoplast DNA replication and early morphological events in the cell cycle of *Trypanosoma brucei*. *J Cell Sci* 95:49–57.
25. Engstler M, et al. (2005) The membrane-bound histidine acid phosphatase TbMBAP1 is essential for endocytosis and membrane recycling in *Trypanosoma brucei*. *J Cell Sci* 118:2105–2118.
26. Henley GL, Lee CM, Takeuchi A (1978) Electron microscopy observations on *Trypanosoma brucei*: Freeze-cleaving and thin-sectioning study of apical part of flagellar pocket. *Parasitol Res* 55:181–187.
27. Bardele CF (1981) Functional and phylogenetic aspects of the ciliary membrane: A comparative freeze-fracture study. *Biosystems* 14:403–421.
28. Smith DS, Njogu AR, Cayer M, Jarlfors U (1974) Observations on freeze-fractured membranes of a trypanosome. *Tissue Cell* 6:223–241.
29. Tetley L (1986) Freeze-fracture studies on the surface-membranes of pleomorphic bloodstream and in vitro-transformed procyclic *Trypanosoma brucei*. *Acta Trop* 43:307–317.
30. Yoshikawa H, et al. (1990) Freeze-fracture study of the bloodstream form of *Trypanosoma brucei gambiense*. *J Protozool* 37:27–32.
31. Linder JC, Staehelin LA (1977) Plasma membrane specializations in a trypanosomatid flagellate. *J Ultrastruct Res* 60:246–262.
32. Vickerman K, Tetley L (1990) in *Ciliary and Flagellar Membranes*, ed Bloodgood RA (Plenum, New York), pp 267–304.
33. Chanez AL, Hehl AB, Engstler M, Schneider A (2006) Ablation of the single dynamin of *Trypanosoma brucei* blocks mitochondrial fission and endocytosis and leads to a precise cytokinesis arrest. *J Cell Sci* 119:2968–2974.
34. Kirchhausen T (2000) Three ways to make a vesicle. *Nat Rev Mol Cell Biol* 1:187–198.
35. Brown KN, Armstrong JA, Valentine RC (1965) The ingestion of protein molecules by blood forms of *Trypanosoma rhodesiense*. *Exp Cell Res* 39:129–135.
36. Suzuki K, Sheetz MP (2001) Binding of cross-linked glycosylphosphatidylinositol-anchored proteins to discrete actin-associated sites and cholesterol-dependent domains. *Biophys J* 81:2181–2189.
37. Berriman M, et al. (2005) The genome of the African trypanosome *Trypanosoma brucei*. *Science* 309:416–422.